

Scaling of Direct Drive Robot Arms

Blake Hannaford, Pierre-Henry Marbot*, Pietro Buttolo, Manuel Moreyra,

Steven Venema

Department of Electrical Engineering, Box 2500

University of Washington, Seattle, WA 98195-2500,

blake@ee.washington.edu

* Now with EdF, Paris

ABSTRACT

This paper studies the ways that the performance of direct drive serial robots changes as system size is changed. We are particularly interested in the physical laws for scaling down direct drive arms to small sizes. Using theoretical scaling analysis, we show that there is a net physical performance advantage to small direct drive arms. A key factor for direct drive robot performance is the torque to mass ratio of the actuators, U . We show how U varies with the scale of DD actuators, and we also calculate how the dynamic

performance varies with scale and U . We compare our calculations with experimental measurements of actuators of various sizes taken from small hard disk drives and compare them with published data for larger motors. Finally, we describe a prototype, 5-axis, direct drive, serial arm having a reach of 10cm and a workvolume of about 136cm^3 . Some potential applications are briefly discussed.

INTRODUCTION

Serial kinematic chains have made up the majority of robot manipulator designs. Serious difficulties with serial mechanisms have proven difficult to overcome. High torques must be generated in the joints due to relatively long moment arms. Hydraulic actuators gave high force to weight ratios, but introduced maintenance and safety concerns. Electrical drives using gear trains, shafts, and couplings, could provide the necessary joint torques. However, these driving components introduced friction which reduced force control capabilities, and backlash which reduced precision. Manipulator stiffness is also reduced by these drive components which are sometimes introduced to reduce the inertia of the links.

Direct drive (DD) serial manipulators were introduced in the 1980's as a proposed solution to many of these problems [Asada and Kanade, 1983, Asada and Youcef-Toumi, 1987, Khosla, 1988, Kazerooni, 1989]. These arms were envisioned as manufacturing manipulators without the above-mentioned deficits of serial kinematic chain manipulators. Because of their intended application on the factory floor, these arms were built on approximately the scale of the human arm.

Direct drive robots had their own sets of difficulties. Chief among these was the high power dissipation required in the motors in order to counteract the acceleration of gravity or other steady state loads. This power dissipation resulted in high coil temperatures which challenged the state of the art in motor design. Another problem of DD arms was that the joint mounted motors tend

to be bulky (i.e. their radius is large compared to the link length) which limits joint motion range and therefore workvolume.

Two approaches have been taken in response to these problems, improvement in transmissions, and improvements in DD motors. Improvements in transmissions include cable drives (Salisbury, et al., 1989) and more precise, limited ratio, gear trains with integrated sensor elements (Khatib and Roth, 1991).

Hollerbach et al.,(1991) have studied actuator capabilities and limitations in detail. They found that a key figure of merit for DD actuators is the specific torque (torque per unit mass). They found that commercially available DD actuators had typical specific torque values of around 3 NM/kg and derived a theoretical limit of 6 NM/kg. They also have reported their design of a water-cooled DD actuator achieving specific torque of up to 10 NM/kg (Hollerbach et al., 1993).

As derived in Hollerbach et al. (1991), in Marbot, (1991), and in Pelrine and Bush-Vishniac (1987) the fundamental limit on specific torque is the ability to dissipate heat generated resistively in the coil windings. Many of the factors governing this heat dissipation depend strongly on the physical scale of the device. Because various elements of physical systems scale differently as the dimensions are scaled, it is not trivial to predict the properties of systems such as actuators and serial arms as the physical dimensions are changed. Trimmer and Jebens (1989) derived scaling laws for force to mass prop-

erties of electromagnetic actuators, but did not extend the results to torque to mass, and more importantly, made a simplistic thermodynamic assumption. Recently, Salcudean and Yan (1994) have published a scaling analysis similar to ours but again did not extend the analysis to specific torque, nor to the total arm system.

Scale analysis has a rich history in science. In the nineteenth century, Froude and Reynolds derived indices of dynamic similarity to relate the performance of scale models to full sized ships (see Lewis, 1988). Froude also derived scaling laws for the speed and range of steamships based on the scaling properties of heat exchangers, fuel bunkers, and fluid resistance (Thompson, 1942). D'Arcy Thompson (1942) derived scaling laws for biomorphology and showed, for instance, that the range of jumping heights for legged animals varies much less than the body mass of the animals (i.e. fleas and humans have about the same jumping height). Recently, Alexander (1991) used scaling arguments to estimate the running speed of dinosaurs based on their fossilized footprints using the fact that the relative running speed depends on the Froude number, $\frac{v^2}{gl}$. Wallace (1993, 1994) has recently analyzed some scaling properties of moving magnet motors which we discuss below. And Pelrine and Bush-Vishniac (1987) have recently studied scaling properties of electromagnetic actuators.

The purpose of this paper is to examine the effects of physical size scale on the dynamic performance of serial chain, DD robots. We will examine the

effects of scale on both DD actuators, and on the integrated system formed by the actuators and the robot arm itself. We will introduce the performance characteristics of small actuators from hard disk drives and briefly describe a 5 degree of freedom (DOF) DD robot arm with total link length of 10 cm recently constructed in our laboratory to evaluate the feasibility of small DD robot arms.

ACTUATION

Theory of heat dissipation

We will now look at properties of magnetic actuators as their size is decreased. The problems that might be experienced include insufficient heat dissipation, low torque output and flux leakage. The following calculation will be based on a practical example, the voice coil actuator (Figure 1).

In the following analysis, we will use scaling theory to determine how the performance of a voice coil actuator will scale as it is made smaller. In scaling theory, we take a set of equations describing a physical system, and assume that the independent variables are either constant or that they vary in proportion to a known power of scale. This variation with scale can either be due to physical law and geometry (such as the dependence of wire resistance on the cross-sectional area) or due to human design (such as a design rule which might arbitrarily vary applied current according to the square of the system dimen-

sion). The scale dependence of the dependent variables can then be computed.

This assumes that the geometry of the magnetic circuitry can be scaled uniformly. However, in practical actuators, the magnetic gap dimension is made as small as possible. Its size will tend to be at the limit of manufacturing tolerance which is constant as opposed to scaled. We will ignore this in the following analysis. However, our intent is to eventually apply the scaling results to large scale changes which inherently require changes in manufacturing methods. Hopefully the derived scaling laws will hold across manufacturing methods if not within them.

We will use the following notation: a variable is expressed with a capital letter if it represents an absolute value (which can change with the size of the system), and with a lower case letter if it represents a normalized value with respect to a power of the scale (for example energy (E) compared to energy density ($e = \frac{E}{S^3}$)). In the following list, we define the variables with their associated normalized variable in parenthesis: S is the system's size (expressed in meters), F (f) is the force generated by the system, P (p) is the electric power, Pd is the power which can be dissipated as heat at a specified temperature, J (j) is the current density¹, I (i) the current, N is the number of turns in the coil, R (r) is the coil resistance, B (b) is the magnetic field from the permanent magnet.

1. This seems confusing since current density is already normalized by area. However, we will later vary current density with scale to keep coil temperature constant.

The force exerted in a moving coil actuator of radius S is given by:

$$F = 2\pi BSNI \quad (1)$$

For simplicity, we will assume $N = 1$ without loss of generality. If we want the system dynamic performance to be invariant, then $F = f S^3$ so that the dynamic behavior of the system is independent of its mass. If we use a permanent magnet to supply B , the magnetic field is a constant which can be expressed as $B = b$. These conditions can be achieved by noting that

$$I \propto JS^2 \quad (2)$$

giving

$$F \propto 2\pi bSJS^2 \quad (3)$$

$$F = fS^3 \quad (4)$$

where we assume a constant value of current density, $J = j$. The electric power can be calculated as follows:

$$P = RI^2 \quad (5)$$

$$\propto R(JS^2)^2 \quad (6)$$

$$= Rj^2S^4 \quad (7)$$

The resistance, R , of a wire is

$$R = \rho \frac{l}{A} \quad (8)$$

where ρ is the resistivity, l , is the length, and A is the cross-sectional area. Since resistivity is a constant property of the material,

$$R = rS^{-1} \quad (9)$$

giving

$$P \propto rS^{-1}j^2S^4 \quad (10)$$

$$P = pS^3 \quad (11)$$

Thus, when current density is constant, the electrical power dissipated in the coil scales just like the force. A useful parameter of motors is the thermal resistance, R_{TH} . Thermal resistance is defined by

$$R_{TH} = \frac{(T_c - T_r)}{P_d} \quad (12)$$

where T_c , and T_r are respectively the coil and room temperatures. We will now see how heat dissipation varies with scale. To do this, we will follow the reasoning of Ron Pelrine and Ilene Bush-Vishniac (1987). To represent convection from the coil surface, we assume that the heat dissipation is proportional to the temperature difference times the square of the scale. Thus,

$$R_{TH} = r_{TH}S^{-2} \quad (13)$$

giving:

$$P_d = \frac{(T_c - T_r)S^2}{r_{th}} \quad (14)$$

If the fundamental performance limit is failure of the actuator due to high temperatures, then we must keep T_c constant as the device is scaled by requiring thermal equilibrium,

$$P = P_d \quad (15)$$

Using (6) and (14),

$$R(JS^2)^2 = r_{th}^{-1}(T_c - T_r)S^2 \quad (16)$$

$$rS^{-1}J^2S^2 \propto r_{th}^{-1}(T_c - T_r) \quad (17)$$

$$J = jS^{-1/2} \quad (18)$$

Using (3),

$$F \propto bjS^{-1/2}S^3 \quad (19)$$

$$F = fS^{2.5} \quad (20)$$

This result is the same as in Salcudean and Yan (1994), but Trimmer and Jebens (1989) obtained $F = fS^2$. The source of this difference lies in their assumption that the surface temperature of the conductor is equal to the ambient temperature. However, it is more reasonable to assume, as we did in (13) and as Salcudean and Yan (1994) did, that the thermal resistance limit is due to convection from the surface (S^2) and not conduction in the copper.

We now consider the torque to mass ratio, U , which is a crucial parameter for direct drive robot dynamic performance (see below). First,

$$\tau = Fl = tS \quad (21)$$

Then using (4) and (20), we get

$$U = \frac{Fl}{M} = \frac{fS^{3.5}}{mS^3} = uS^{1/2} \quad (22)$$

To summarize this key result, as the actuator size is changed, if the coil winding temperature is held constant, the ratio of maximum torque to mass varies with the square root of the system scale. In particular, this implies that as actuators are scaled down, their performance in direct drive robots will diminish.

Wallace (1994) has made a similar calculation based on a "quality factor",

$$Q = \frac{K_M}{M} \quad (23)$$

where the motor constant is defined by

$$K_M = \frac{F}{\sqrt{P}} \quad (24)$$

where P is the electrical power. His analysis showed that

$$Q = qS^{-1/2} \quad (25)$$

but these results do not explicitly consider a constant upper temperature limit.

Experimental Measurements Relevant to Scaling of Hard Disk Drive Actuators

One factor which slows the progress in robotics research is that manufacturing volumes of robots are low. Direct drive robots are made in even lower volumes. In contrast, in some industries, the large production volume justifies extensive engineering efforts towards optimization of every aspect of the product's design. Hard disk drives are a high volume product with stringent requirements for actuation which are in many ways similar to those of direct drive robots. The heads must be positioned over the disk surface with great precision and their acceleration must be precisely controlled in an open-loop manner through torque trajectories. Also, as a result of new portable applications and competitive pressure from the makers of solid state memories, disk drives have been continuously miniaturized for about 20 years (Figure 2). We wondered if the above scaling laws would be evident in flat-coil actuators taken from disk drives since they appear to be essentially identical actuators

driven down a scaling path and presumably optimized by competition and market forces.

Disk drives use several different types of actuators for positioning their heads. The main types are stepping motors, voice coil motors, rotary voice coil motors, and flat coil motors. Flat coil motors (Figure 3) work by winding a single coil of wire around an axis parallel to the axis of rotation of the actuator. The coil is wedge shaped, and placed in a gap formed by two oppositely polarized magnets in such a way that one arm of the coil is always adjacent to one polarization and the other arm to its opposite. This configuration produces a net torque because each leg of the coil lies in a magnetic field of opposite polarity. However, the motion range of these actuators is typically limited to 20-40 degrees.

We made engineering tests on flat coil head positioning actuators taken from hard drives of sizes ranging from 5.25" to 1.8" media diameter (Buttolo et al., 1994). This 4:1 range of linear dimensions corresponds to a 64:1 range of volumes and therefore masses, which serves our purpose here. Second, hard disk drives contain many precision mechanical parts which may prove useful in the design of small, accurate, DD robots. All of the actuators had the same flat-coil geometry (Figure 3). However, two additional actuators were tested: a 1.8" actuator with only a single magnet on one side of the coil, and a double magnet 1.8" actuator in which we filled the magnetic gap and surrounded the coil with

ferrofluid (type EMG905, Ferrofluidics Corp, Nashua NH, 03061-2009)

METHODS

Hard disk drives were obtained from local repair shops and manufacturers. We measured coil temperature with type "T" thermocouples bonded to the coil surface with thermally conductive epoxy. Electrical variables were measured using digital volt-ohm meters. We measured torque using a digital force gauge at a known lever arm from the axis of motion. All temperature measurements are reported in the steady state. The devices had thermal time constants on the order of 5-10 minutes.

For these motors, the torque produced is linearly proportional to coil current and almost independent of position. The "maximum" torque is really a thermal limit determined by the temperature at which the insulation will fail (Curie temperatures were not approached). A usual standard is to measure torque with a current sufficient to raise the temperature of the coil to a specified value. We measured coil temperature as a function of coil current twice; once with the actuator coil in free air and once with the actuator installed in the drive. The values reported are for the coil mounted in the drive case. R_{TH} is the temperature rise divided by the electrical power.

Using the torque constant, K_t , it is possible to estimate the static friction level for the actuators. We started from zero and gradually increased current without an external load until a deflection of the actuator was observed.

The torque required to visibly deflect the actuator was a function of position. Our measurement reports the average value of this torque for three positions across the range of motion.

Mass was obtained by weighing the coil, actuator body, magnets and frame. The drive case, media, heads, and head arms were not included.

Volume was measured by wrapping the actuator parts tightly in plastic, immersing them in water, and observing displacement.

To obtain a value for "maximum" torque output, an operating temperature must be selected. This should be based on the temperature rating of the insulation material which was unavailable to us. We used an arbitrary value of 200 degrees Fahrenheit (111 deg. C) above ambient temperature. This temperature did not cause any observable change in the actuators and corresponded to an absolute coil surface temperature of 137 deg C, comparable to the value used by Hollerbach et al. (1992).

In addition to the direct measurements, we derived R_{TH} and U for the actuators we tested. We also plotted them against equations representing the scaling trends derived above. This comparison must be made cautiously since we could not verify that all aspects of the actuators we tested were in fact scaled uniformly as assumed in the analysis. For example, we could not verify that the magnets were all of the same material.

RESULTS

The measurements we made on the actuators are reported in Table 1. The actu-

Table 1: Flat Coil Actuator Properties

| Drive Size | Mass [gr] | Vol. [cm ³] | R T ₀ =27°C [ohm] | Static Friction [Nm*10 ⁻³] | Torque ΔT=111°C [Nm*10 ⁻³] | R _{TH} [°C/Watt] | Torque/ Mass [Nm/Kg] |
|------------|-----------|-------------------------|------------------------------------|---|--|------------------------------|----------------------------|
| 5.25" | 237 | 111 | 21.6 | 0.33 | 57.4 | 11.1 | 0.24 |
| 3.5" | 65 | 27 | 26.9 | 0.22 | 18.6 | 15.8 | 0.29 |
| 2.5" | 41 | 28 | 16.8 | 0.05 | 18.8 | 32.6 | 0.46 |
| 1.8" dm | 22 | 9 | 6.5 | 0.07 | 8.9 | 24.0 | 0.40 |
| 1.8" sm | 14 | 9 | 6.2 | 0.07 | 6.8 | 22.1 | 0.48 |
| 1.8" ff | 22 | 9 | 6.5 | N/A | 11.1 | 15.4 | 0.50 |

ator masses varied over a 10:1 range. Maximum torques varied from 57.4×10^{-3} Nm to 6.8×10^{-3} Nm from the largest to smallest actuator. Minimum torque (indicating the static friction level) was typically about 100 times less than the maximum torque.

Derived Measures

We calculated the thermal resistance of the actuators (Table 1, Figure 4).

We have also plotted an equation,

$$R_{TH} = \frac{184}{D^2} \quad (26)$$

To compare the trend against that expected from equation (13).

Following Hollerbach et al., 1992, we computed the specific torque by divid-

ing maximum torque by mass. These values ranged from 0.242 Nm/kg for the 5.25" drive to 0.50 Nm/kg for the double magnet 1.8" actuator with added ferrofluid. These values are low with respect to the approximate theoretical limit of 6.0 derived in Hollerbach et al. because of the flat coil geometry. In the flat coil geometry, only a fraction of the total magnetic flux is used to generate force (Figure 3). The ratio of magnet area to coil area in the actuators tested was between 4:1 and 5:1. If new coils were wound to use the entire magnet area, they would increase the torque by this ratio without significantly increasing mass. This would give specific torques in the range of 1.0 to 2.5 Nm/kg, comparable to commercially available large DD actuators. According to our previous calculations,

$$U = uS^{1/2} \quad (27)$$

The specific torque measured for these actuators can plotted against media diameter (Figure 5). In contrast to the result predicted by the preceding scale analysis, U increased with reduction of disk media diameter (see discussion). The data were reasonably well fit by

$$U = \frac{0.6}{\sqrt{D}} \quad (28)$$

To get a rough idea of the maximum permissible operating temperature, we performed a "smoke test" on one of the 2.5" drives. We gradually increased the temperature of the coil by increasing applied current. We observed a small amount of smoke at 155 deg C. With the available power supply, we were able to

increase the temperature to about 250 degrees C with 12 watts of power. The smoke rate did not substantially increase. Upon re-cooling the device, no change in resistance was measurable.

Ferrofluidic materials have been used occasionally in voice coils in high frequency loudspeakers. We injected type EMG905 oil based ferrofluid into the magnetic gap of the double magnet 1.8" drive. The added conduction path for heat flow, and perhaps a small reduction in flux leakage, resulted in the peak torque increasing by about 25%. The mass of the added fluid was less than 1 gram.

Upon injection, the ferrofluid neatly filled the magnetic gap, immersing most of the coil. After the ferrofluid was added, the actuator showed a noticeable attraction for the ends of its motion range without any applied current. The torque required to move the actuator from the limits was 0.7×10^{-3} Nm. This was due to the fact that at the extremes of motion, certain parts of the coil frame extended beyond the magnetic gap. Thus at the motion extreme, less ferrofluid was displaced from the gap, and the total system energy was reduced.

SERIAL ARM DYNAMICS

One of the most basic functions of a serial robot arm is to hold itself and its payload up against gravity. A major part of the weight of direct drive

robot arms is the actuators which in turn defines torque requirements for the proximal joints. Is there a minimum value of specific torque below which the arm cannot hold itself against gravity?

To study this question, consider the schematic planar chain of direct drive actuators and links in Figure 6. Assume the link length is l , link structure mass is zero, and a payload of mass m_0 is attached to the end effector. For this analysis it is convenient to number the links in increasing order from the end effector to the base in contrast to the usual practice. Let U be the specific torque, that is the ratio of torque to mass in the actuators. Wallace (1994) has studied similar simplified "finger" and "leg" robots, but assumed equal mass for all actuators.

The torques in the actuators are

$$\tau_1 = m_0gl \quad (29)$$

$$\tau_2 = m_1gl + m_0g2l \quad (30)$$

$$\tau_3 = m_2gl + m_1g2l + m_0g3l \quad (31)$$

where g is the acceleration of gravity. These can be written as a series

$$\tau_j = gl \sum_{i=0}^{j-1} (j-i) m_i \quad (32)$$

We further assume that the arm is designed to have the minimum actuator torque sufficient for resisting gravity in the position shown¹, and that motors of any torque capability are available, and that for a given design, the spe-

1. An arbitrary level of performance can be achieved with this approach by using a higher value for the acceleration of gravity than actually present.

cific torque, U is constant for all motors in the serial chain (see discussion). The masses are then related to the torques by:

$$m_j = \frac{\tau_j}{U} \quad (33)$$

Substituting this into the torque series, (32),

$$\tau_j = \frac{gl}{U} \sum_{i=0}^{j-1} (j-i) \tau_i, \quad (34)$$

with the initial value

$$\tau_0 = Um_0 \quad (35)$$

This is a Fibonacci-like series which grows very quickly with j . However, the torques and masses are always finite as long as U is non zero.

Thus, no matter how small U is, the arm can, in principle, be designed to stand up to gravity if the motors are allowed to grow in size rapidly enough from distal to proximal. The non-moving mass of the base motor can be made arbitrarily large to allow enough torque at the base.

In a practical case, of course, it is necessary to limit the mass and volume of the actuators. To take this into account, a useful measure of performance can be formed from the ratio of the payload mass to the base actuator mass. To study this performance measure, it is useful to go back to the case of three links and motors (Figure 6). Using (34) and (35), we get

$$\tau_3 = m_0 g \left(3l + \frac{4gl^2}{U} + \frac{g^2 l^3}{U^2} \right) \quad (36)$$

giving

$$\frac{m_0}{m_3 u} = \frac{1}{g \left(3l + \frac{4gl^2}{U} + \frac{g^2 l^3}{U^2} \right)} \quad (37)$$

or

$$\frac{m_0}{m_3} = \frac{1}{3\alpha + 4\alpha^2 + \alpha^3} \quad (38)$$

where

$$\alpha = \frac{gl}{U} \equiv \text{arm index} \quad (39)$$

α is thus a dimensionless measure of *dynamic similarity* of direct drive robot arms. Equation (38) shows that all arms which have the same α have the same dynamic performance and that performance varies inversely with α . Furthermore, lower values of U are required for smaller direct drive serial robots if performance is constant. Alternatively, small versions of direct drive arms which preserve U , will have correspondingly greater performance. To illustrate this phenomenon, we can consider a few numerical examples (Table 2) which compare the payload ratio for three-link DD robots having link lengths of 0.3 m, 0.03m and 0.01 m, and having actuators with U ranging from 0.3 to 15 Nm/kg. These link lengths were selected to represent a typical industrial sized direct drive manipulator ($l = 0.3m$), a robot typical of the DD prototype described below ($l = 0.03m$), and a hypothetical ultra-mini robot ($l = 0.01m$).

We can see that a small robot using motors with a relatively low specific torque of $U = 0.5$ has the same arm index and therefore performance as a large robot using the specific torque expected of the new water cooled motors,

Table 2: 3-link calculated performance comparison

| U | $l = 0.01m$ | | $l = 0.03m$ | | $l = 0.3m$ | |
|-----|-------------|-------------------|-------------|-------------------|------------|-----------------------|
| | α | $\frac{m_0}{m_3}$ | α | $\frac{m_0}{m_3}$ | α | $\frac{m_0}{m_3}$ |
| 15 | 0.0065 | 50.6 | 0.0196 | 16.6 | .196 | 1.33 |
| 10 | 0.0098 | 33.6 | 0.0294 | 10.9 | .294 | 0.798 |
| 6 | 0.016 | 20.4 | 0.0490 | 6.38 | .490 | 0.392 |
| 3 | 0.033 | 9.67 | 0.098 | 3.000 | 0.98 | 0.129 |
| .5 | 0.196 | 1.33 | 0.588 | 0.299 | 5.89 | 0.0028 |
| .3 | 0.33 | 0.684 | 0.980 | 0.130 | 9.80 | 7.38×10^{-4} |

$U = 15$ (Hollerbach et al., 1992).

Now, let us combine the two scaling results. We have seen that arm performance varies inversely with α . Substituting (27) into (39) we get,

$$\alpha = aS^{1/2} \quad (40)$$

Thus, the overall performance improves for smaller arms. The exact form of the scaling law depends on the number of links. For the three link case, it is obtained by substituting (40) into (38).

MINI DIRECT DRIVE ROBOT PROTOTYPES

Two recently developed mini direct drive robots (Marbot, 1991, Marbot & Hannaford, 1991, Hannaford et al., 1994a) were built to test the feasibility of small DD arms. Their joints are actuated by a set of disk drive actuators

decreasing in size towards the end-effector. The arm has a work volume of about 50 cc and has 5-10 micron or better resolution and repeatability. A more detailed description of the mini robot and its performance is available in Moreyra, et al., 1995.

MINI-ROBOT MECHANISM

The first axis actuator is a linear voice coil from a 5.25 inch hard disk drive. The second joint is driven by a rotary magnetic actuator. The third axis actuator is a rotary voice coil. The body of the mini-robot contains 20 individual parts machined of aluminum and anodized.

Biomedical applications, such as electrophoresis procedures and laboratory sample manipulation, were used as a guideline in the robot's development. An additional goal was to produce a device suitable to act as a slave manipulator for experiments in scaled force reflection (Colgate, 1991, Hannaford, 1991, Kobayashi & Nakamura, 1992, Hwang and Hannaford, 1994). The project attempts to extend the technology of mini-robotics with several particular emphases:

- Employ direct drive actuation to maintain accuracy and repeatability, to enhance force control and to avoid backlash.
- Provide good dynamic performance by minimizing inertia.
- Use miniature disk-drive components, to get high precision, low inertia and low cost.
- Make the two orientation axes intersect at the wrist.

WORKSPACE DESIGN

The mini-robot workspace is reduced to an unusual extent by the limited range of the disk drive rotary actuators. Optimization of the performance of the mini-robot involved obtaining as large a work space as possible without compromising speed, force and precision of end effector movements. The work space chosen was approximately 80 mm. height, 68 mm. width and 25 mm. length. This will allow the robot to reach about 18 of the wells on a standard 96 well microtiter plate. This will be sufficient for experimental biomedical laboratory applications. The workvolume is approximately 136 cm^2 .

The overall design of the first three axes is the same in both prototypes. However, for the second prototype (Hannaford et al., 1994a) the parts have been re-designed and re-machined to improve precision and to support the addition of two more motion axes. The same linear voice coil actuator was used for the first, linear motion axis. Two high accuracy, low friction linear ball bearings, also taken from disk drives, guide and support the first motion axis.

The second joint is driven by a rotary magnetic actuator. Its angular stroke is $\pm 15^\circ$ and the arm is 6" (152mm) long, giving a Y-axis travel of ± 1.55 " (± 40 mm.). The third axis actuator has angular stroke of $\pm 13^\circ$ giving a Z-axis travel of ± 1.35 " (± 34 mm.).

The fourth and fifth joints have $\pm 20^\circ$ of stroke. We do not consider them to affect work volume since they drive intersecting axes at the wrist. However, there is a minimum offset from wrist center to tool mount of 22 mm. Due to the

low torque of actuator 3 and the relatively high weight and size of the actuator and encoder used on the fifth joint, direct drive in the strict sense of the term is not used. Instead, a cable and two pulleys are used to drive this joint with a 1:1 mechanical advantage.

A novel aspect of this remote direct drive arrangement is that the actuator for joint 5 is mounted on link 3 instead of link 4. This provides lower inertia for actuator 3. Motion of joint 4 causes a slight length change of the transmission cable. This is accommodated by using an aramid fiber for the cable. The compliance of the belt is low enough that the natural frequency of joint 5 is still above 200Hz (Moreyra, 1994). A US patent is pending on this design.

MINI-ROBOT KINEMATICS

The mini robot forward kinematic model is derived using the Denavit-Hartenberg convention and the frame definitions used in Craig (1991). Figure 8 depicts the schematic link diagram on which the kinematic analysis (Table 3) is based.

SENSORS

Most robots today use digital incremental position encoders to estimate

Table 3: Mini-robot Denavit-Hartenberg parameters.

| i | a_{i-1} (degrees) | a_{i-1} (mm.) | d_i (mm.) | q_i (degrees) |
|---|------------------------|--------------------|----------------|---------------------|
| 1 | 0 | 0 | $d_1 = \pm 12$ | 0 |
| 2 | -90 | 0 | 0 | $q_2 = -90 \pm 15$ |
| 3 | -90 | 12.5 | 0 | $q_3 = -60 \pm 13$ |
| 4 | -90 | 0 | 152 | $q_4 = 180 \pm 20$ |
| 5 | -90 | 0 | 0 | $q_5 = -120 \pm 20$ |

joint positions. This works well when the mechanism design allows several turns of the encoder disk for small joint motions. However, the direct drive feature of the mini-robot, coupled with the desire for small, very high-precision motions, implies the need for different position measurement approaches.

LVDT Position sensor

For joint 1, a linear variable differential transformer (LVDT) is used. A specialized monolithic IC is used for the LVDT signal conditioning (Signetics NE5521). In our implementation, a 12-bit A/D converter effectively limits the LVDT resolution to 1 part in 4096. The 1-inch travel of joint 1 therefore implies a position measurement precision of $0.0254m/2^{12} = 6.2\mu m$. This was verified in the earlier prototype by microscopic inspection of the axis displacement (Marbot & Hannaford, 1991).

Analog Incremental Encoders

Joints 2-5 are instrumented with analog incremental rotary position encoders. Unlike digital encoders, these encoders output two analog, continuous, periodic, waveforms, in roughly quadrature phase. These analog outputs allow a

high degree of interpolation between each encoder line (Marbot, 1991, Venema, 1994). However, the actual outputs from most analog encoders are far from the ideal sinusoidal form. Phase differences of 110° are not uncommon. When plotted against each other, these signals make an irregular potato-like shape instead of the expected perfect circle. The *potato algorithm* (Marbot, 1991) was developed to address these non-ideal behaviors of the encoder signals. Space limitations preclude more detailed treatment. For more details see (Marbot, 1991). An improved auto calibration method based on Kalman filter estimation has recently been developed (Venema, 1994).

POWER ELECTRONICS

Most full-scale robots today are driven by pulse-width modulation (PWM) power electronics. The popularity of PWM is due primarily to its ability to control large amounts of power (up to several kilowatts per joint) with very high efficiency. However, the high-speed current switching used in PWM systems generates a large amount of electromagnetic interference (EMI) and often objectionable acoustic noise. Digital sensors (e.g., digital incremental encoders) can be made to operate robustly in this type of environment using good shielding and grounding techniques. However, to get less than 1-bit of noise on our analog to digital conversions, we must have a signal-to-noise ratio of better than 74dB. The amount of EMI generated by PWM power electronics makes it dif-

difficult to shield the encoder signals sufficiently to achieve this desired SNR.

Since the power levels needed to actuate the mini-robot are relatively small (~50 watts peak per actuator), we used linear power amplifiers to drive the voice-coil actuators. High-power op-amps were configured as voltage controlled current sources for each joint. D/A converters on our computer control system directly control the motor currents.

COMPUTER SYSTEM

A real-time digital computer system is used to control the mini-robot. The computer is an in-house design based upon Texas Instrument's TMS320C30 DSP chip. The processor consists of a 6U-VME form-factor circuit board containing the 32 MHz DSP chip, up to 256k 32-bit words of high speed SRAM, a special bus for communications with other processor boards, a daughter-card bus for the addition of peripheral cards, and an RS232-compatible serial communications port for interface with an external host computer. Each daughter card contains 4 separate 33kHz 12-bit A/D and 12-bit D/A channels as well as 8 bits of digital input and 16 bits of digital output. Up to four daughter cards may be stacked on a single processor board. Details of this design, including the processor's Neural Broadcast communications bus, can be found in MacDuff et.al, (1992). The system configuration is shown in Figure 9.

DISCUSSION

This paper has described research studying the fundamental properties of small direct drive robots. We have analyzed the scaling properties of electromagnetic actuators as well as the scaling of the dynamics of serial chain direct drive robot arms. The first scaling analysis showed that torque to mass ratio, U , of direct drive actuators degrades as actuators get smaller by the factor of $S^{1/2}$. The second analysis assumed that U can be held constant over the chain and showed that there is an index of dynamic similarity

$$\alpha = \frac{gl}{U}$$

for direct drive serial chains, and that dynamic performance varies inversely with α in a way which depends on the number of joints opposing gravity (see eqn (38) for the case of three joints). Thus, as the robot gets smaller, dynamic performance improves.

To summarize, the performance of DD arms improves as they are scaled to smaller sizes because the dynamics of the arm itself improves faster than the torque-to-mass ratio of the actuators degrades.

In holding U constant throughout the serial chain, we have ignored the relation between motor size and U derived in the first section. This was done to simplify the analysis. In doing so, we have made a conservative assumption

with regard to dynamic performance. In actuality, an arm such as that of figure 6 would have larger motors for the more proximal joints which would in turn have higher values of U according to equation (27). Thus, dynamic performance will exceed that predicted by equation (38).

We should note that non-gravity-loaded inertias, such as rotational inertias of the motor, and inertias due to counterbalancing, have not been taken into account. Thus this analysis is limited to the static case of gravity loading.

Using the conservative assumption above, (40) shows that performance improves for small DD arms, but the scaling dependence (power law) is actually a polynomial, and thus a single power dependence cannot be identified. It can however be approximated if parameters such as length scale are known.

Unlike robot arms, computer hard disk drives are sold in the millions each year. This volume justifies extensive engineering effort devoted to scaling and optimization. We wondered if this competitive pressure results in actuators who's properties follow the theoretical scaling trends given the basic flat-coil design (Figure 3).

The actuators we tested did not follow the scaling laws we derived in spite of their very similar (but scaled) physical appearance. However, we could not verify that all of their physical properties were in fact the same. For example, we don't know if the same magnetic alloys were used, whether or not the

magnet volume *really* varied with S^3 , etc.

To verify the performance and explore possible uses for mini DD robotics, we built a prototype 5-axis mini DD robot about 10 cm in length which is now operational in our laboratory. Our current prototype has not fully realized the advantages revealed in the scaling analysis. Although our robot is capable of resisting gravitational loads, great care was taken to minimize those loads through location of the actuators and a novel two-joint actuation scheme (Hanaford et al., 1994a, Moreyra 1994).

The actuators we used have torque to mass ratios roughly one tenth of those used in previous full sized DD robots. Although we have not yet fully characterized its performance, the 5-axis prototype has no problems maintaining a stable pose under 1-g gravity load and moving around freely in all directions. To accomplish this, we have used many design methods similar to those in full sized DD robots:

- Axes one and two are not loaded by gravitational acceleration.
- Axis three is approximately balanced: actuator 4 balances the end effector mass.

Actuator 5 is remotely located, attached to link 3, near the center of mass. Much better dynamic performance can be realized through the development of modified actuators having significantly higher torque to mass ratios. We plan to develop these actuators by winding multi-phase flat coils, combining magnets from existing disk-drive actuators, and possibly employing newer magnetic

materials and ferrofluids.

Our scaling analysis of multi-link arms involved several simplifications. One of these is that we neglected the mass of the sensors. In human sized DD arms, this assumption is justified. For a given level of end point sensing resolution, the required angular resolution scales with S . However in building our prototype, we were not able to find small sensors which scaled in anything close to proportion to link length. As a result, the mass and volume of joint angle sensors is very significant in our prototype. Total moving sensor mass was 118 gr. out of a total moving mass of 815 gr. or 15% (Moreyra, 1994). Unfortunately, disk drive technology does not come to the rescue because positioning feedback in working disk drives comes from information read from the magnetic media.

We feel that the potential for small direct-drive robots is very great. Biomedical applications include scaled teleoperation for dexterous micro-surgery with force feedback, laboratory automation of ultra-low volume sample handling, and high performance micro-manipulators for traditional applications such as electrophysiology and DNA micro-injection.

We also foresee industrial applications. For example, the new PCMCIA interface standard for personal computer expansion cards consists of surface mounted ICs on a card about the size of a credit card. A miniaturized assembly cell could be built with a small direct drive arm having just enough workvolume to reach over the PCMCIA card and a few parts feeders for chips. The low cost and

space requirements of such a system could open whole new niche products to cost effective manufacturing.

The arm forms an initial prototype for the NASA/University of Washington MicroTrex flight telerobotics experiment (Hannaford, et al., 1994b). In this proposed space flight experiment, a mini DD robot will be launched into low earth orbit and teleoperated from a ground station on earth to investigate the potential of mini robots in space teleoperation.

ACKNOWLEDGEMENTS

This work was supported by the National Science Foundation, PYI Grant BCS-9058408, the University of Washington Royalty Research Fund, the Washington Technology Center, and by donations of 1.8" disk drives by Integral Peripherals, Longmont Co. We are grateful for useful discussions with Prof. Richard Wallace.

REFERENCES

Alexander, R.M., 1991, "How Dinosaurs Ran", Scientific American, v264, n4, pp 130-137.

Asada, H., T. Kanade, 1983, "Design of Direct-Drive Mechanical Arms," ASME

J. Vibration, Acoustics, Stress, and Reliability in Design, vol. 105, pp. 312-316.

Asada, H., K. Youcef-Toumi, 1987, "Direct Drive Robots, Theory and Practice," Cambridge, MA, MIT Press.

Buttolo, P., D.Y. Hwang, B. Hannaford, 1994, "Experimental Characterization of Hard Disk Actuators for Mini Robotics," Proc. SPIE Telemanipulator and Telepresence Technologies Symposium, Boston.

Colgate, J.E., 1991, "Power and Impedance Scaling in Bilateral Manipulation," Proc. IEEE Intl. Conf on Robotics and Automation, pp. 2292-2297, Sacramento, CA.

Craig, J., 1991, "Introduction to Robotics: Mechanics and Control," Addison Wesley, 2nd Edition, 1991.

Hannaford, B., 1991, "Kinesthetic Feedback Techniques in Teleoperated Systems," In "Advances in Control and Dynamic Systems", C. Leondes, Ed., Academic Press, San Diego.

Hannaford, B., P.H. Marbot, M. Moreyra, S. Venema, 1994a, "A 5-Axis Mini Direct Drive Robot for Time Delayed Teleoperation," Proc. Intelligent Robots and Systems (IROS 94), Munich.

Hannaford, B., S. Venema, A.K. Bejczy, 1994b, "MICROTREX: Micro-Telerobotic Flight Experiment," Proceedings AIAA Space Programs and Technologies Conference; AIAA 94-4509, Huntsville, Alabama.

Hollerbach, J.M., I.W. Hunter, J. Ballantyne, 1991, "A Comparative Analysis of Actuator Technologies for Robotics," In "The Robotics Review", O. Khatib, J. Canny, T. Lozano-Perez, Ed., MIT Press.

Hollerbach, J.M., I. Hunter, J. Lang, S. Umans, R. Sepe, E. Vaaler, I. Garabieta, 1993, "The McGill/MIT Direct Drive Motor Project," Proceedings IEEE Intl. Conf. on Robotics and Automation, vol. 2, pp. 2.611-2.617, Atlanta, GA.

Hwang, D.Y., B. Hannaford, 1994, "Modeling and Stability analysis of a Scaled Telemanipulation," Proceedings RO-MAN 94, Nagoya, Japan.

Kazerooni, H., 1989, "Design and Analysis of the Statically Balanced Direct-Drive Manipulator," IEEE Control Systems Magazine, vol. 9, no. 2, pp. 30-34.

Khatib, O., B. Roth, 1991, "New Robot Mechanisms for New Robot Capabilities," Proc. IEEE/RSJ Intl Workshop on Intelligent Robots and Systems IROS'91, pp. 44-49, Osaka Japan.

Khosla, P.K., 1988, "Some Experimental Results on Model-Based Control Schemes," Proc. IEEE Intl. Conf. on Robotics and Automation, vol. 3, pp. 1380-1385, Philadelphia, PA.

Kobayashi, H., H. Nakamura, 1992, "A Scaled Teleoperation," Proc. IEEE Intl Workshop on Robot and Human Communication, pp. 269-274, Tokyo, Japan.

Lewis, E.V., 1988, "Principles of Naval Architecture," vols. 1-3, Society of Naval Architects and Marine Engineers, Jersey City, NJ.

MacDuff, I., S. Venema, B. Hannaford, 1992, "The Anthroform Neural Controller: An Architecture for Spinal Circuit Emulation," Proceedings of IEEE International Conference on EMBS, pp. 1289,90, Paris, France.

MacDuff, I., S. Venema, B. Hannaford, 1992, "The Anthroform Neural Controller: A System for Detailed Emulation of Neural Circuits," Proceedings, IEEE International Conference on Systems, Man, and Cybernetics, Chicago, IL.

Marbot, P.H., 1991, "Mini Direct Drive Robot for Biomedical Applications," MSEE Thesis, University of Washington, Department of Electrical Engineering.

Marbot, P.H., B. Hannaford, 1991, "Mini Direct Drive Arm for Biomedical Applications," Proceedings of ICAR 91, pp. 859-864, Pisa, Italy,.

Moreyra, M.R., 1994, "Design of a Five Degree of Freedom Direct Drive Mini-Robot Using Disk Drive Actuators," Masters Thesis, University of Washington, Department of Mechanical Engineering.

Moreyra, M.R., P.H. Marbot, S. Venema, B. Hannaford, 1995, "A 5-Axis Mini Direct Drive Robot for Time Delayed Teleoperation," In "Intelligent Robots and Systems 1994", V. Graefe, Ed., Elsevier Science.

Pelrine, R., I. Bush-Vishniac, 1987, "Magnetically Levitated Micro-Machines," Proceedings, IEEE Micro Robots and Teleoperators Workshop.

Salisbury, J.K., B. Eberman, M. Levin, W. Townsend, 1989, "The design and control of an experimental whole-arm manipulator.," In "Robotics Research. Fifth International Symposium.", H. Miura and S. Arimoto, Ed., MIT Press,

Tokyo, Japan.

Thompson, D'Arcy, 1942, "On Growth and Form," Cambridge University Press.

Venema, S.C., 1994, "A Kalman Filter Calibration Method for Analog Quadrature Position Encoders", MSEE Thesis, University of Washington, Department of Electrical Engineering.

Wallace, R.S., 1993, "Miniature Direct Drive Rotary Actuators," Robotics and Autonomous Systems, vol. 11, no. 2, pp. 129-33.

Wallace, R.S., 1994, "Building and Interfacing Miniature Direct Drive Actuators," Tutorial Notes, International Conference on Robotics and Automation, San Diego, CA.

Figure Captions

Figure 1.

Architecture of a voice coil actuator.

Figure 2.

Size reduction trend in computer hard disk drives. Log media diameter is plotted against year of introduction (author's recollection). The trend is fit well by 10% per year reduction in diameter (dashed line). The crossed out circle marks a failed product introduction.

Figure 3.

Dimensions of a flat coil head positioning actuator from a 1.8" disk drive. the magnet (hatched region) has two regions of polarity so that each leg of the coil generates force in the same direction.

Figure 4.

Thermal resistance for hard drive actuators.

Figure 5.

Specific torque of head actuators vs. disk drive media diameter. The data points are reasonably well characterized by an inverse square root law in contrast to the expected theoretical limitation (see text).

Figure 6.

Simplified schematic diagram of a direct drive serial arm resisting gravitational torques

Figure 7.

Photograph and drawings of the Mini Direct Drive Robot.

Figure 8.

Mini robot schematic diagrams. Kinematic linkage diagram (a) and side view of mechanism and workspace (b).

Figure 9.

Control system block diagram.

Figure 1

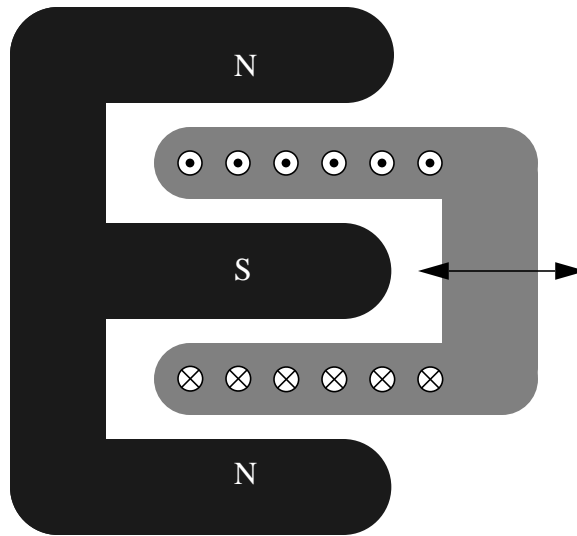


Figure 2

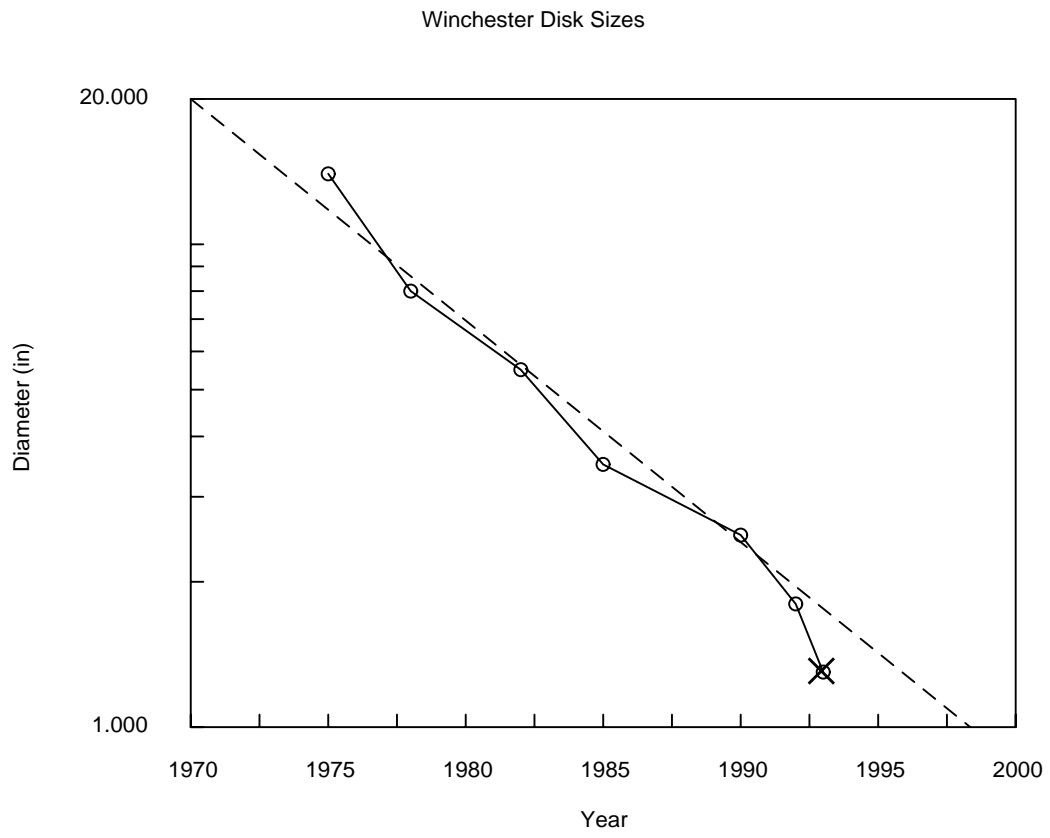


Figure 3

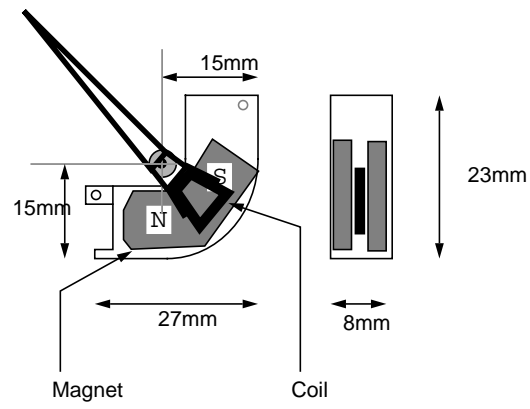


Figure 4

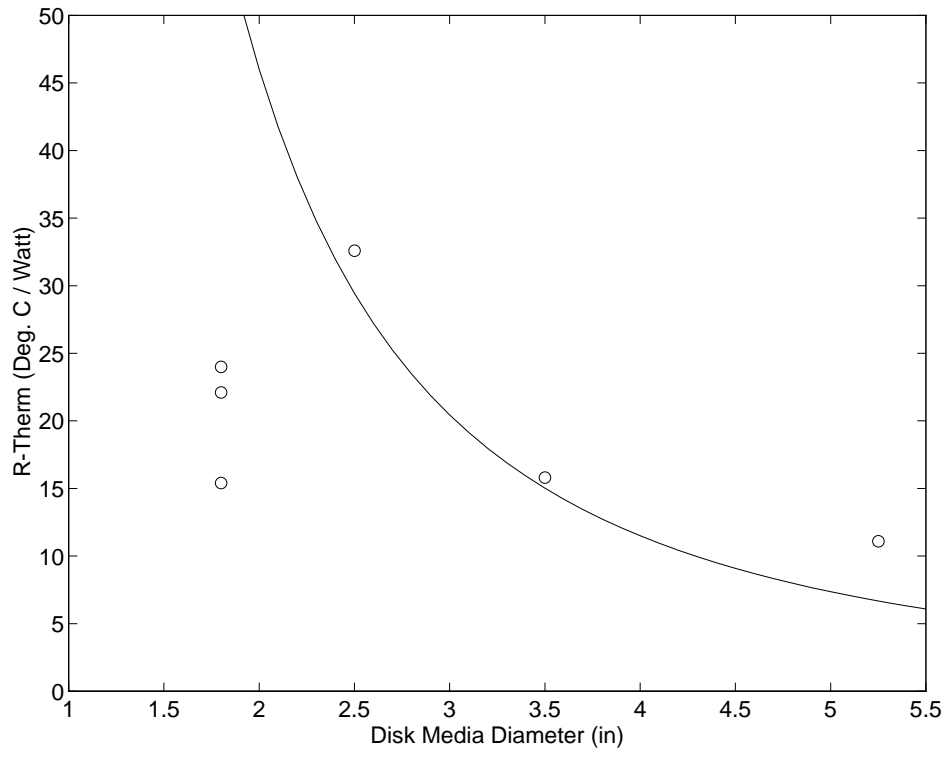


Figure 5

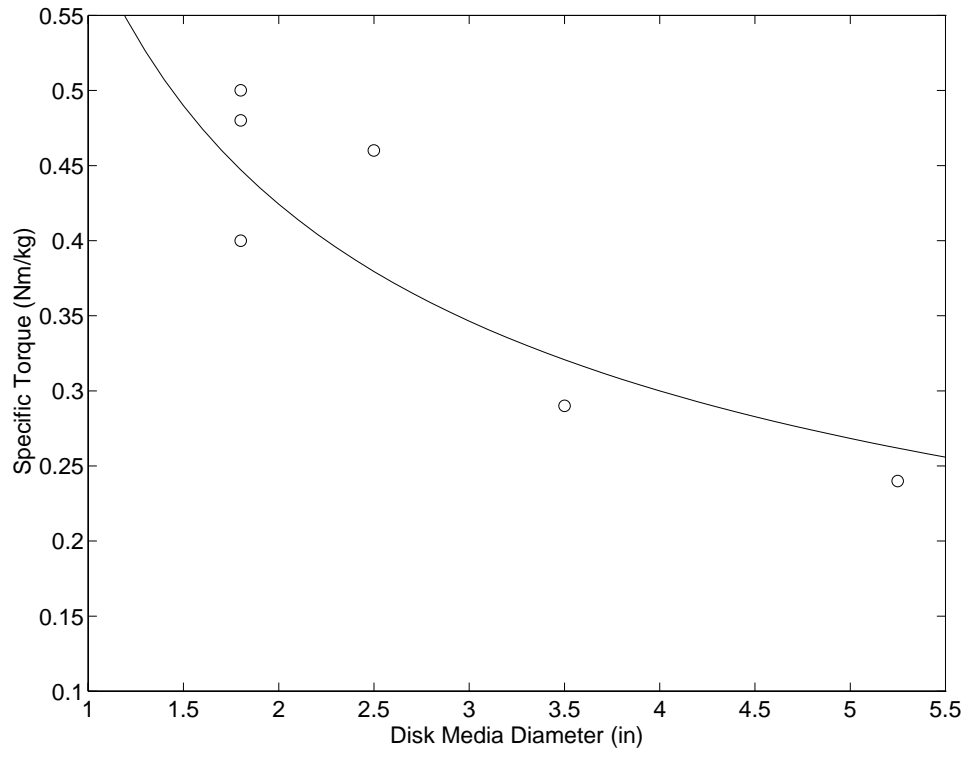


Figure 6

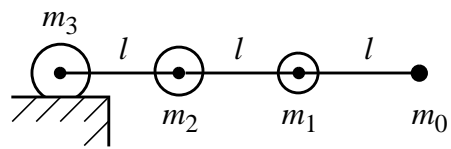


Figure 7

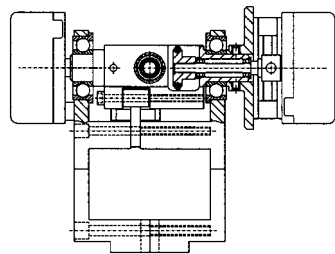
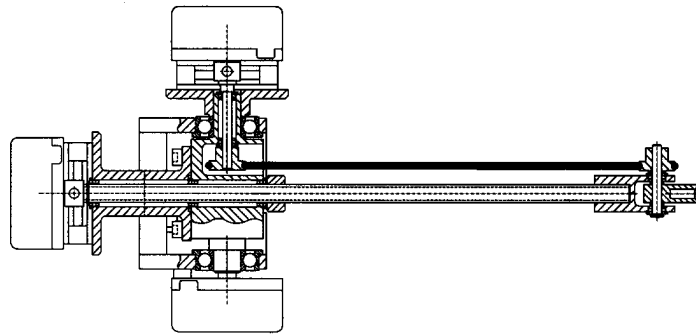
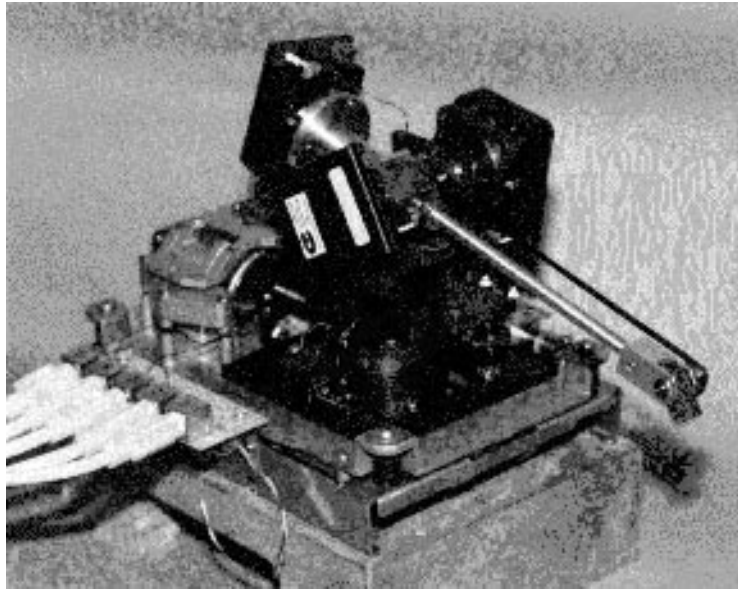


Figure 8

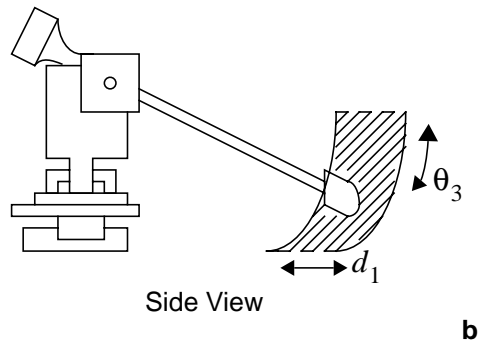
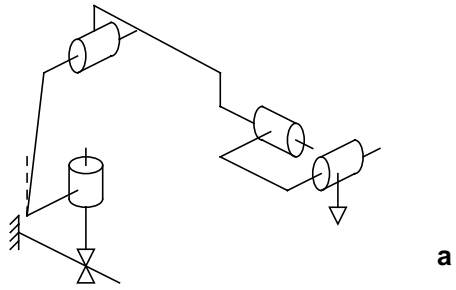


Figure 9

